

Polarization effect on critical power and luminescence in an air filament

Chang Liu (刘畅), Hongwei Zang (臧宏伟), Helong Li (李贺龙), Yanhao Yu (于颜豪),
and Huailiang Xu (徐淮良)*

State Key Laboratory on Integrated Optoelectronics, College of Electronic Science and Engineering,
Jilin University, Changchun 130012, China

*Corresponding author: huailiang@jlu.edu.cn

Received June 14, 2017; accepted October 13, 2017; posted online November 2, 2017

We demonstrate that the filamentation process is strongly influenced by the polarization state of the driver laser. When the laser polarization changes from linear to circular, the critical power for the self-focusing of a Ti:Sapphire laser (800 nm, 40 fs) in air increases from about 9.6 ± 1.0 to 14.9 ± 1.5 GW, while the second nonlinear refractive index n_2 of air decreases from 9.9×10^{-20} to 6.4×10^{-20} cm²/W. We also demonstrate that the luminescence from the neutral nitrogen molecules at 337 nm is dependent on both the laser intensity and plasma density inside the filament.

OCIS codes: 020.2649, 300.6280, 260.5950, 260.5210, 190.3270.
doi: 10.3788/COL201715.120201.

Laser-induced filamentation is a unique nonlinear phenomenon that has attracted a lot of interest since the first experimental observation of a self-guided plasma channel in 1995^[1]. Filamentation generated by the most popular Ti:Sapphire femtosecond laser in air can be attributed to a dynamic interplay between Kerr self-focusing and defocusing of the plasma generated by multiphoton/tunneling ionization^[2]. Due to the unique properties of ultrahigh clamping intensity and a long self-guided plasma channel, laser-induced filamentation has shown many potential applications, including terahertz (THz) radiation generation^[3-6], combustion diagnosis^[7], generation of air laser^[8-12], atmospheric sensing^[13-16], and so forth. However, laser-induced filamentation is a highly nonlinear process and, thus, sensitive to the experimental conditions, such as external focusing condition^[17], initial beam radius^[18], and laser pulse duration and polarization^[19,20], which unavoidably lead to a strong effect on a variety of phenomena associated with laser filamentation. For example, it was demonstrated recently that fluorescing and lasing generated in filaments can be strongly influenced by the polarization states of the driver laser^[21,22].

On the other hand, it is well-known that filamentation occurs when the driver laser power exceeds a so-called critical power for self-focusing. Therefore, the critical power is considered one of the most fundamental physical parameters in the filamentation process and has been extensively investigated so far^[2]. For instance, it was found that the critical power changes from 10 to 5 GW in air when the pulse duration of an 800 nm driver laser increases from 42 to 200 fs^[19], and that the critical power is sensitive to the propagation media, e.g., ~ 268 GW in helium gas^[23] and ~ 2.2 GW in combustion flame^[24] for 800 nm and 40 fs laser pulses at atmospheric pressure. The dependence of the critical power for self-focusing on the polarization states has also been previously

demonstrated for solid material by using chirped pulses with pulse durations in the nanosecond range^[25]. However, to the best of our knowledge, the critical power for self-focusing of the ultrafast femtosecond driver laser with different polarization states in air has not been experimentally determined yet; although, it is commonly accepted that the critical power should be higher for the self-focusing of a circularly polarized light than that of a linearly polarized light^[25,26]. Due to less nonlinearity contribution from the nuclear response for an ultrafast femtosecond laser pulse^[19], direct measurement of critical power for self-focusing of a few 10 fs pulses with different polarization states would provide more insights into the nonlinear properties of molecules in ultrafast intense light fields.

In the present study, we experimentally measure the critical power of different polarized lasers in air by observing the shift of the laser focal position as a function of the driver laser energy. This method is based on the fact that when the laser power exceeds the critical power, self-focusing occurs, leading to the focal position moving toward the laser source; while when the laser power is smaller than the critical power, the focal position would not change^[19]. Based on the measured critical powers, we investigate the variation of the luminescence signals of nitrogen molecules produced during the filamentation of linearly and circularly polarized lasers in air under a single filament condition. We find that along the propagation axis of the filament, the fluorescence from the $C^3\Pi_u - B^3\Pi_g$ transition of N₂ at 337 nm and that from the $B^2\Sigma_u^+ - X^2\Sigma_g^+$ transition of N₂⁺ at 391 nm shows different behaviors and demonstrates that these phenomena can be influenced by both the plasma density and laser intensity inside the filament.

The experiment was performed using a Ti:sapphire femtosecond laser system (Spectra Physics, Spitfire)

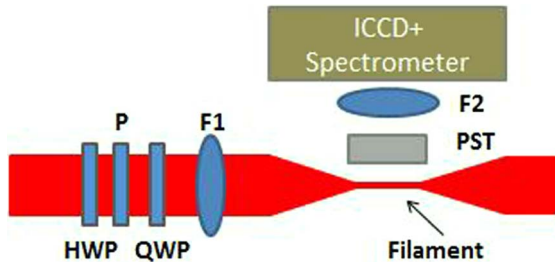


Fig. 1. Schematic diagram of the experimental setup. P, polarizer; F1, fused silicon lens with $f = 1$ m; PST, periscope system; F2, fused silicon lens with $f = 6$ cm.

producing ~ 40 fs pulses with the central wavelength at 800 nm and the repetition rate at 1 kHz. Figure 1 shows the experimental apparatus used for the critical power measurement. A half-wave plate (HWP, Thorlabs AHWP05M-980) and a polarizer were used to control the laser energy. A quarter-wave plate (QWP, Thorlabs AQWP05M-980) was installed after the polarizer to control the polarization of the laser pulse, and a fused silicon lens ($f = 1$ m) was placed after the QWP to focus the laser pulse directly in air. A single plasma channel (filament) was produced, whose length depends on the input energy and the laser polarization. The laser beam diameter before the focal lens is about 10 mm. A periscope system was prepared to collect the fluorescence perpendicularly to the propagation direction of the laser beam, so that the plasma channel (filament) can be aligned to be parallel to the entrance slit of the spectrometer (Andor Shamrock SR-303i). A fused silicon lens ($f = 60$ mm, diameter = 50.8 mm) was used to focus the filament onto the entrance slit of the spectrometer equipped with an ICCD (Andor iStar). The fluorescence from the filament was imaged on the ICCD camera. With this apparatus, the plasma channel produced with the laser power compared to the critical power can be totally imaged by the ICCD camera so that the shift of the focal position of the laser beam can be monitored. The entrance slit width of the spectrometer was set to be 100 μm . The ICCD gate width and delay of the ICCD were set to $\Delta t = 200$ ns, and $t = -10$ ns, respectively. Note that $t = 0$ is the arrival time of the laser pulse at the interaction zone.

For the investigation on the variation of the luminescence signals of nitrogen molecules produced by the linearly and circularly polarized lasers with higher input energies, the periscope was removed, and instead a fused silicon lens ($f = 60$ mm, diameter of 50.8 mm) was used to collect the fluorescence from the filament in a $2f$ - $2f$ manner. The fused silicon lens ($f = 1$ m) that produced the filament was placed on a moving stage, so that, by moving the 1 m focal lens, the fluorescence along the propagation axis of filament can be collected.

Shown in Fig. 2 are the typical spectra induced by the filamentation of linearly and circularly polarized 40 fs laser pulses in air. Both the linearly and circularly polarized pulse energies were 1.8 mJ. The spectral bands can be assigned to

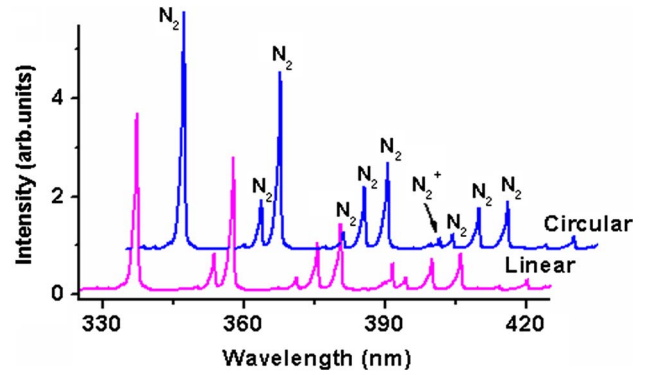


Fig. 2. (Color online) Typical spectra induced by the filamentation of linearly and circularly polarized femtosecond laser pulses in air.

different vibrational level transitions between the $C^3\Pi_u$ and $B^3\Pi_g$ states of N_2 and those between the $B^2\Sigma_u^+$ and $X^2\Sigma_g^+$ states of N_2^+ ^[13,14]. In Fig. 3, we show the measured focal position of the linearly and circularly polarized laser pulses as a function of laser energy, respectively. Note that the smaller value in the Y axis represents the closer distance of the focal position to the focal lens. The focal position of the laser pulse in Fig. 3 was determined, in a similar way as those shown in Refs. [19,24], by recording the luminescence at 337 nm for the $C^3\Pi_u - B^3\Pi_g$ transition from neutral nitrogen molecules along the laser propagation direction.

It can be clearly seen from Fig. 3 that there are two different regions, that is (i) the focal position stays almost constant when the input laser energy is smaller than a certain value; (ii) the focal position moves toward the focal lens when the input laser pulse becomes larger than this value. This can be interpreted based on the combined contributions of the external focusing and the self-focusing to the input laser beam^[20],

$$1/f' = 1/f + 1/z_f, \quad (1)$$

where f represents the focal length of external focusing lens, and z_f is the self-focusing distance of a collimated Gaussian beam. When the peak power exceeds the critical power, the self-focusing distance can be determined by the empirical formula^[26],

$$z_f = \frac{0.367ka^2}{\{[(P/P_{\text{cr}})^{1/2} - 0.0852]^2 - 0.0219\}^{1/2}}, \quad (2)$$

with k being the wave number, a is the radius of the beam profile at the $1/e$ level, P is the input laser power, and P_{cr} is the critical power. Therefore, when the peak power exceeding the critical power further increases, the focal spot of the laser beam will move towards the external focal lens. Whereas when the peak power of the laser pulse is smaller than the critical power, the contribution from self-focusing would be zero, leading to the unaltered focal position of the laser beam at the geometrical focus of the external

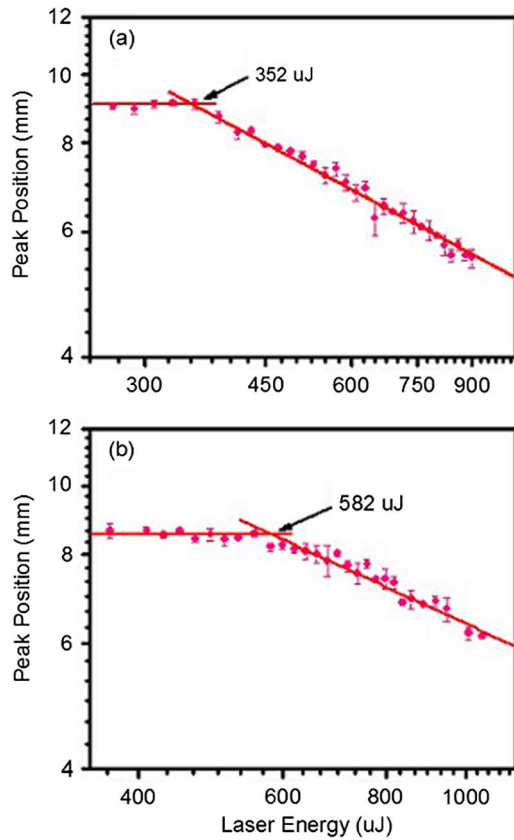


Fig. 3. Peak position of the 337 nm signal as a function of input laser energy of (a) linearly and (b) circularly polarized laser pulses. The solid lines are linear fits to the experimental results.

focal lens. Consequently, by linearly fitting the data in these two regions in Fig. 3, it can be seen that the energies at the cross point of the lines are 352 and 582 μJ for Figs. 3(a) and 3(b), respectively. With the pulse duration of 40 fs, the critical powers in air are determined to be 8.8 and 14.55 GW for self-focusing of the linearly and circularly polarized pulses in air, respectively.

We further measured the critical power with different polarization states of the laser pulse, as shown in Fig. 4. The angles in the x axis represent different polarization states with 0° and 90° being the linear polarization, 45° being the circular polarization, and other values being the elliptical polarizations with different ellipticities. All of the critical powers were measured in the same way, as shown in Fig. 3, by observing the shift of the focal spot as a function of input laser energy. As can be seen from Fig. 4, the critical powers obtained with elliptically polarized pulses are in between the linear and circular cases. By fitting the data in Fig. 4 with a sinusoidal function, the critical powers for the self-focusing of the linearly and circularly polarized pulses are determined to be 9.6 ± 1.0 and 14.9 ± 1.5 GW, respectively.

The critical power measured in this work for self-focusing of the linearly polarized pulse agrees well with the previous measurement of 10 GW^[19]. It can also be noted that the critical power for self-focusing of the

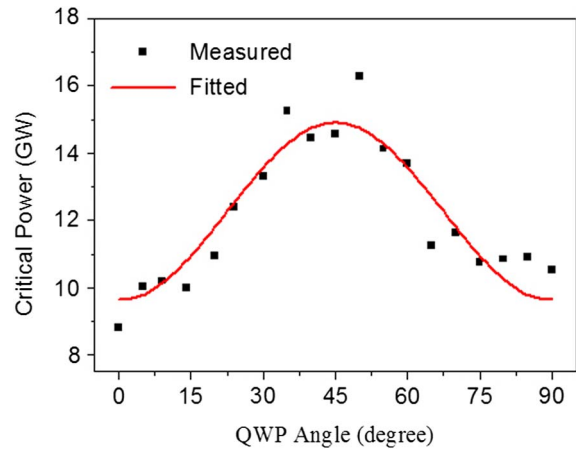


Fig. 4. Critical powers measured with different pump laser polarizations. The horizontal axis represents the rotation angle of the QWP.

circularly polarized light is much larger, showing the intrinsic nature that the second-order nonlinear index coefficient n_2 in an optical medium is smaller for circularly polarized light than for linearly polarized light. According to the relation of $P_{\text{cr}} = 3.72 \lambda^2 / (8\pi n_0 n_2)$, where n_0 and λ are, respectively, the linear index of the refraction coefficient of air and the pump laser wavelength^[26], the second-order nonlinear index coefficients of the air for the used linear and circular polarization pulses (800 nm, 40 fs) are deduced to be $n_2 = 9.9 \times 10^{-20} \text{ cm}^2/\text{W}$, and $n_2 = 6.4 \times 10^{-20} \text{ cm}^2/\text{W}$, respectively ($n_0 = 1$ in air). This value of $n_2 = 9.9 \times 10^{-20} \text{ cm}^2/\text{W}$ is in good agreement with the result ($12 \times 10^{-20} \text{ cm}^2/\text{W}$ for 800 nm, 90 fs laser pulses) measured by a polarization technique^[27]. In addition, it can be noted that the second-order nonlinear index coefficients of air for the linear polarization pulse is ~ 1.5 times higher than that for the circularly polarized light, which is in good agreement with the theoretical prediction^[26].

Furthermore, it is found that as the input laser energy increases the luminescence signals at 391 and 337 nm induced by the linearly and circularly polarized pulses show different behaviors. In Fig. 5, we show the signal distributions of the 391 and 337 nm luminescence along the propagation axis produced by the circularly (green circle) and linearly (red square) polarized laser pulses with three laser energies of 0.7, 1.2, and 1.8 mJ, respectively. In all three cases, the powers of linearly and circularly polarized light are higher than their critical powers, and a signal filament condition is preserved. It can be clearly seen from Figs. 5(a)–5(c) that for all the three input energies, the laser pulses with linear polarization are more efficient for inducing the luminescence at 391 nm from nitrogen molecular ions. It is well-known that the ionization rate of nitrogen molecules is much higher (1–2 orders of magnitude) for linearly polarized than circularly polarized light of the same intensity at the level of $1 \times 10^{14} \text{ W}/\text{cm}^2$ ^[28]. The clamped intensity in the linearly

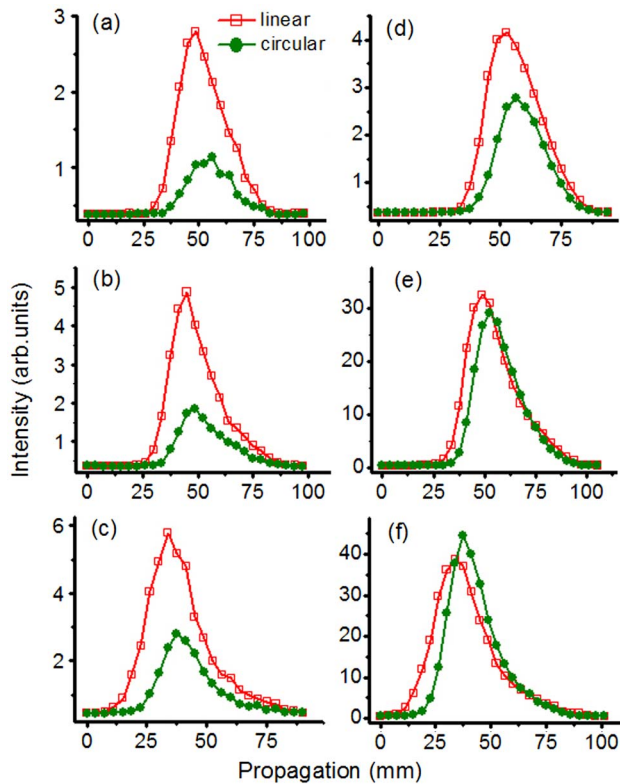


Fig. 5. (Color online) Spatial evolution of (a)–(c) 391 nm and (d)–(f) 337 nm produced by linearly and circularly polarized laser pulses with the laser energy of (a) and (d) 0.7 mJ, (b) and (e) 1.2 mJ, and (c) and (f) 1.8 mJ. The focal length is $f = 1$ m.

polarized light filament can be estimated to be 1×10^{14} – 2×10^{14} W/cm² with an f-number of 100–150^[29], and that in the circularly polarized light filament should be 1.5 times higher, according to the measured critical powers^[30]. However, the clamped intensity difference could not reverse the ionization rates of these two laser polarization cases, which conforms to theoretical calculations^[28]. Thus, the experimental observation that the 391 nm fluorescence is always stronger for linearly than circularly polarized laser filaments verifies that strong-field-induced ionization (including ionization-dependent^[31]) processes are dominant in a single filament case for producing the 391 nm signals. On the other hand, it can be noted in Figs. 5(a)–5(c) that the ratio of the 391 nm signal produced by circularly and linearly polarized pulses increases as the laser energy increases, which may result from the different contributions from the plasma densities that vary differently for the linearly and circularly polarized pulses as the laser energy increases^[17].

Nevertheless, unlike the luminescence phenomena shown in Figs. 5(a)–5(c), it can be seen from Figs. 5(d)–5(f) that there exists a reversal in the relative intensity of the 337 nm luminescence between the linear and circular polarizations as the laser energy increases. Similar behaviors of the 337 nm luminescence reversal in filaments have also been previously reported^[22,32], in which it was explained that upon the increase of the input laser energy, electrons

induced by the circularly polarized laser pulses are accelerated away from the molecular ion, and their kinetic energies can be high enough to produce the excited state $C^3\Pi_u$ of N_2 when the laser energy is larger than a certain threshold^[22]. However, it has not been convincingly explained why the electrons could gain more energy with the almost constant clamped intensity inside a filament, that is, it is questioned why, with the almost constant or slightly changed clamped intensity in the filamentation condition, the electron energy could not change significantly to induce the reversal behavior of 337 nm luminescence.

Here, we propose that both the plasma density and the laser intensity play important roles in the observed reversal phenomenon. So far, the mechanisms proposed for the 337 nm luminescence can be summarized as follows: (i) the collision reaction $N_2^+ + N_2 \rightarrow N_4^+$ followed by $N_4^+ + e \rightarrow N_2(C^3\Pi_u) + N_2$ processes with an electron density of $>1 \times 10^{15}$ cm⁻³^[33]; (ii) the collision-assisted intersystem crossing with an electron density on the order of 1×10^{13} cm⁻³^[34]; (iii) the electron impact excitation in the case of circular polarization^[22]. When the laser power (higher than the critical power) is lower, it is undoubted that the first two collision mechanisms that have higher probabilities in generating the 337 nm signals with linear polarization are dominant, owing to the stronger 337 nm signal shown in Figs. 5(d)–5(e). When the laser energy increases with the generation of a single filament ($P \geq P_{cr}$), the laser intensity in the filament is clamped to an almost constant value^[29], which will give rise to an almost matching electron kinetic energy distribution. However, it was demonstrated that the plasma density could slowly increase as the input power increases^[17], and if the input power further increases ($P \gg P_{cr}$), multiple filaments or superfilaments occur, giving rise to even one order of magnitude denser plasma^[35], and, thus, a larger probability of electron impact for stronger 337 nm luminescence in the case of circular polarization. That is, as the input laser energy increases, although the electron energy kinetic distribution keeps almost the same due to the almost constant (or slightly changed) clamped intensity, the increased electron density can significantly increase the electron impact probability and, thus, enhance the 337 nm signals, leading to the reverse behavior of the 337 nm luminescence.

In addition, it was shown that a tight focus can produce a much higher clamped intensity inside the filament than a loose focus^[29]. This will lead to a higher plasma density^[17] with higher energy electrons^[22], resulting in stronger 337 nm signals even in a lower input laser energy (higher than the critical power). The stronger intensity in the filament by a tight focus can also induce a higher ionization rate, thus a stronger 337 nm signal than that in a loose focus case, which is in contrast to the conclusion that the first two mechanisms could be distinguished based on the experimental results observed with a tight focus^[32]. Furthermore, the reverse behavior of the 337 nm luminescence could be wavelength-dependent. For the case of the driver pulse with a longer wavelength, it is well-known that the

electron accelerated by the circularly polarized pulse will gain more kinetic energy due to the higher ponderomotive energy^[33], which would lead to a higher probability to excite the state $C^3\Pi_u$ of N_2 .

In conclusion, we investigate the influence of the laser polarization on the critical power for self-focusing of femtosecond laser pulses in air, and experimentally measure the critical power for the used linearly and circularly polarized pulses that are 9.6 to 14.9 GW, respectively. Based on the measured critical power, the second-order nonlinear index coefficients of the air are deduced to be ~ 1.5 times higher for the linearly than circularly polarized pulses. We also demonstrate that the luminescence behaviors from the neutral and ionic nitrogen molecules in filaments are strongly influenced by external conditions. The plasma density plays an essential role in the luminescence of neutral nitrogen molecules at 337 nm inside the filament. Our results shed more light on understanding the luminescence mechanisms of nitrogen molecules in air filaments.

This work was supported in part by the National Natural Science Foundation of China (Nos. 61625501, 61427816, and 61235003), the National Basic Research Program of China (No. 2014CB921300), the Open Fund of the State Key Laboratory of High Field Laser Physics (SIOM), and the Program for JLU Science and Technology Innovative Research Team (JLUSTIRT) (No. 2017TD-21).

References

1. A. Braun, G. Korn, X. Liu, D. Du, J. Squier, and G. Mourou, *Opt. Lett.* **20**, 73 (1995).
2. S. L. Chin, *Femtosecond Laser Filamentation* (Springer, 2010).
3. C. D'Amico, A. Houard, M. Franco, B. Prade, A. Mysyrowicz, A. Couairon, and V. T. Tikhonchuk, *Phys. Rev. Lett.* **98**, 235002 (2007).
4. J. L. Liu, J. M. Dai, S. L. Chin, and X. C. Zhang, *Nat. Photon.* **4**, 627 (2010).
5. Y. Bai, L. W. Song, R. J. Xu, C. Li, P. Liu, Z. N. Zeng, Z. X. Zhang, H. H. Lu, R. X. Li, and Z. Z. Xu, *Phys. Rev. Lett.* **108**, 255004 (2012).
6. T. Wang, S. Yuan, Y. Chen, and S. L. Chin, *Chin. Opt. Lett.* **11**, 011401 (2013).
7. H. L. Li, H. L. Xu, B. S. Yang, Q. D. Chen, T. Zhang, and H. B. Sun, *Opt. Lett.* **38**, 1250 (2013).
8. Q. Luo, W. Liu, and S. L. Chin, *Appl. Phys. B* **76**, 337 (2003).
9. J. P. Yao, B. Zeng, H. L. Xu, G. Li, W. Chu, J. Ni, H. Zhang, S. L. Chin, Y. Cheng, and Z. Z. Xu, *Phys. Rev. A* **84**, 051802(R) (2011).
10. D. Kartashov, S. Alisauskas, A. Baltuska, A. Schmitt-Sody, W. Roach, and P. Polynkin, *Phys. Rev. A* **88**, 041805 (2013).
11. S. L. Chin, H. Xu, Y. Cheng, Z. Xu, and K. Yamanouchi, *Chin. Opt. Lett.* **11**, 013201 (2013).
12. K. Zhai, Z. Li, H. Xie, C. Jing, G. Li, B. Zeng, W. Chu, J. Ni, J. Yao, and Y. Cheng, *Chin. Opt. Lett.* **13**, 050201 (2015).
13. H. L. Xu and S. L. Chin, *Sensors* **11**, 32 (2010).
14. H. L. Xu, Y. Cheng, S. L. Chin, and H. B. Sun, *Laser Photon. Rev.* **9**, 275 (2015).
15. H. Xu, R. Li, and S. L. Chin, *Chin. Opt. Lett.* **13**, 070007 (2015).
16. H. Xu, A. Azarm, and S. L. Chin, *Chin. Opt. Lett.* **12**, 113201 (2014).
17. F. Théberge, W. W. Liu, P. T. Simard, A. Becker, and S. L. Chin, *Phys. Rev. E* **74**, 036406 (2006).
18. Q. Luo, S. A. Hosseini, W. Liu, J. F. Gravel, O. G. Kosareva, N. A. Panov, N. Akozbek, V. P. Kandidov, G. Roy, and S. L. Chin, *Appl. Phys. B* **80**, 35 (2005).
19. W. Liu and S. L. Chin, *Opt. Express* **13**, 5750 (2005).
20. S. Rostami, M. Chini, K. Lim, J. P. Palastro, M. Durand, J. C. Diels, L. Arissian, M. Baudelet, and M. Richardson, *Sci. Rep.* **6**, 20363 (2016).
21. H. Zhang, C. Jing, G. Li, H. Xie, J. Yao, B. Zeng, W. Chu, J. Ni, H. L. Xu, and Y. Cheng, *Phys. Rev. A* **88**, 063417 (2013).
22. S. Mityukovskiy, Y. Liu, P. J. Ding, A. Houard, A. Couairon, and A. Mysyrowicz, *Phys. Rev. Lett.* **114**, 063003 (2015).
23. J. Bernhardt, P. T. Simard, W. Liu, H. L. Xu, F. Théberge, A. Azarm, J. F. Daigle, and S. L. Chin, *Opt. Commun.* **281**, 2248 (2008).
24. H. L. Li, W. Chu, H. W. Zang, H. L. Xu, Y. Cheng, and S. L. Chin, *Opt. Express* **24**, 3424 (2016).
25. D. N. Schimpf, T. Eidam, E. Seise, S. Hadrich, J. Limpert, and A. Tunnermann, *Opt. Express* **17**, 21 18774 (2009).
26. J. H. Marburger, *Self-focusing: Theory* (Prog. Quantum Electron, 1975).
27. V. Lorient, E. Hertz, O. Faucher, and B. Lavorel, *Opt. Express* **18**, 3011 (2010).
28. A. Becker, A. D. Bandrauk, and S. L. Chin, *Chem. Phys. Lett.* **343**, 345 (2001).
29. X. L. Liu, W. B. Cheng, M. Petrarca, and P. Polynkin, *Opt. Lett.* **41**, 4751 (2016).
30. S. L. Chin, T. J. Wang, C. Marceau, J. Wu, J. S. Liu, O. Kosareva, N. Panov, Y. P. Chen, J. F. Daigle, S. Yuan, A. Azarm, W. W. Liu, T. Seideman, H. P. Zeng, M. Richardson, R. Li, and Z. Z. Xu, *Laser Phys.* **22**, 1 (2012).
31. H. L. Xu, E. Lotstedt, A. Iwasaki, and K. Yamanouchi, *Nat. Commun.* **6**, 8347 (2015).
32. Y. Shi, A. M. Chen, Y. F. Jiang, S. Y. Li, and M. X. Jin, *Opt. Commun.* **367**, 174 (2016).
33. H. L. Xu, A. Azarm, J. Bernhardt, Y. Kamali, and S. L. Chin, *Chem. Phys.* **360**, 171 (2009).
34. B. R. Arnold, S. Roberson, and P. M. Pellegrino, *Chem. Phys.* **405**, 9 (2012).
35. G. Point, Y. Brelet, A. Houard, V. Jukna, C. Milián, J. Carbonnel, Y. Liu, A. Couairon, and A. Mysyrowicz, *Phys. Rev. Lett.* **112**, 223902 (2014).